# Quasi-One-Dimensional Quantized States in an Epitaxial Ag Film on a One-Dimensional Surface Superstructure

Naoka Nagamura, Iwao Matsuda,* Nobuhiro Miyata, Toru Hirahara, and Shuji Hasegawa
*Department of Physics, School of Science, University of Tokyo, 7-3-1 Hongo, Bunkyo-ku, Tokyo 113-0033, Japan*

Takashi Uchihashi
*National Institute for Materials Science, 1-1 Namiki, Tsukuba, Ibaraki 305-0044, Japan*
(Received 4 April 2006; published 26 June 2006)

The in-plane energy dispersion of quantized states in an ultrathin Ag film formed on the one-dimensional (1D) surface superstructure Si(111)-(4 × 1)-In shows clear 1D anisotropy instead of the isotropic two-dimensional free-electron-like behavior expected for an isolated metal film. The present photoemission results demonstrate that an atomic layer at the film-substrate interface can regulate the dimensionality of electron motion in quantum films.

DOI: 10.1103/PhysRevLett.96.256801 PACS numbers: 73.20.At, 68.65.Fg, 73.63.Hs, 79.60.Dp

Reduction of metal film thickness down to the electron wavelength induces energy quantization by the quantum size effect, resulting in the formation of quantum-well states. Recently, there has been growing interest in such quantum films on solid surfaces [1–4]. In contrast to a freestanding metal film, these quantum-well states (resonances) have been reported to show additionally intriguing physical properties such as spin polarization [5], anomalous in-plane dispersion [6–9], and oscillation of the superconducting transition temperature with thickness [2]. Furthermore, it has been predicted that the Fermi surface topology can be changed by an interface layer (electronic topological phase transition) [10]. Such topological regulation induces various effects of geometry on the physical properties of electrons, attracting interest in low-dimensional physics and technology.

In this Letter, we find a new property of a quantized state in an atomically flat metal film on a semiconductor substrate. When a Ag film has been grown on an array of In chains, the Si(111)-(4 × 1)-In surface [11,12], electron motion in the film is restricted only in one direction parallel to the substrate and the chain direction. The measurements of angle-resolved photoemission spectroscopy (ARPES) have revealed that quantized states show parabolic dispersion along the In chain direction but almost a flat one in the perpendicular direction. Formation of such a quasi-one-dimensional (1D) electronic state is sharply in contrast to previous isotropic quantum-well states in Ag films on clean Si surfaces [6,13], indicating a critical role of the quasi-1D interface layer. Furthermore, discrete energy levels of the quasi-1D state have a lower binding energy than those of the quantum-well states formed in the isotropic Ag film on Si(111)-(7 × 7) with the same film thickness. This can be explained naturally by the additional quantum confinement effect, and it is quantitatively confirmed by the phase-boundary conditions.

The ARPES experiments were done with unpolarized He $I\alpha$ radiation and an electron spectrometer (Scienta SES-100) equipped with angle and energy multidetection. Fermi surfaces and band dispersions were acquired at room temperature by rotating a sample [14]. A regularly stepped Si(111)-(7 × 7) clean surface was prepared on a vicinal Si wafer ($n$-type, 2 ~ 15 Ω cm), whose normal was 1.8° off from (111) toward the $[\bar{1}\,\bar{1}\,2]$ direction, by the appropriate resistive heat treatments [15]. Indium was deposited on this surface at about 350 °C to make a single-domain Si(111)-(4 × 1)-In surface [11,12]. Ultrathin Ag(111) films were epitaxially formed by depositing 15–30 monolayers (ML, 1 ML = 2.36 Å thick) of Ag below 150 K on Si(111)-(4 × 1)-In or Si(111)-(7 × 7), followed by post-annealing at 300–400 K [6,16]. The surface superstructures and thin films were monitored by *in situ* observation of reflection high-energy electron diffraction. Indium chains of Si(111)-(4 × 1)-In run parallel (perpendicular) to the $[1\bar{1}0]$ ($[\bar{1}\,\bar{1}\,2]$) axis of bulk Si, corresponding to the $\bar{\Gamma} - \bar{K}$ ($\bar{\Gamma} - \bar{M}$) direction for the overlayer Ag(111) surface Brillouin zone, respectively. For simplicity of discussion, we define that the $y$ direction is parallel to the In chain direction (∥ In chain) and $x$ perpendicular to the In chain direction (⊥ In chain). The coverage and evaporation rate of Ag were separately determined by the completion of the Si(111)$\sqrt{3} \times \sqrt{3}$-Ag structure [14].

Figure 1(a) shows a series of normal-emission photoemission ($\bar{\Gamma}$) spectra at different amounts of Ag deposition on Si(111)-(7 × 7) and Si(111)-(4 × 1)-In. A large peak of the Ag(111) surface state, denoted as SS, is always found at the vicinity of the Fermi level $E_F$, and its clear appearance indicates formation of atomically flat Ag(111) films. On the other hand, energy levels at a binding energy ($E_B$) of 0.3–2 eV are attributed to quantized states by quantum confinements in the films along the surface normal ($z$ direction), and the wave vectors obey the boundary condition (phase-accumulation model [3,5,17]):

$$\phi_{\mathrm{vac}} + 2k_z^{\mathrm{env}} d + \phi_{\mathrm{sub}} = 2\pi n, \qquad (1)$$

where $n$ is the quantum number, $k_z^{\mathrm{env}}$ is the wave vector of

 

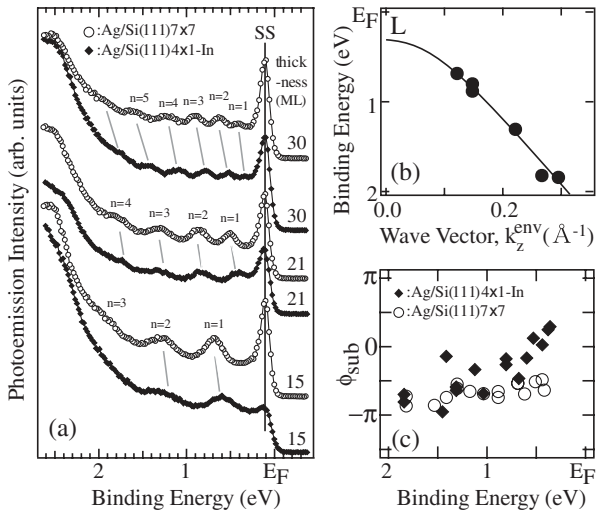


FIG. 1. (a) Normal-emission ARPES spectra of Ag films with various thickness on Si(111)-(7 × 7) (open circles) and Si(111)-(4 × 1)-In (solid diamonds) surfaces. The peak positions of the Ag(111) surface state (SS) and quantized states are assigned. (b) The $sp$-band dispersion for Ag films along the surface normal direction ($\Gamma - L$ line). The solid circles are the experimental points taken from Ag films on Si(111)-(4 × 1)-In. The solid curve is a least-squares fit based on the two-band nearly free-electron model. (c) Change of the phase shift at the film-substrate interface $\phi_{sub}$ for the Ag films on Si(111)-(4 × 1)-In (solid diamonds) and on Si(111)-(7 × 7) (open circles) as a function of the binding energy.

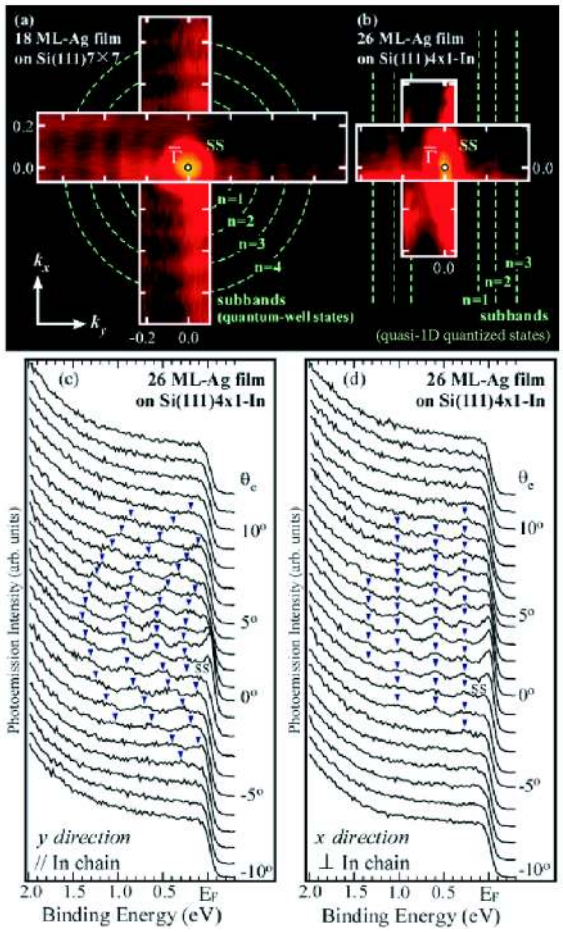


FIG. 2 (color online). (Upper) Photoemission intensity maps at $E_F$ of Ag quantum films prepared on (a) Si(111)-(7 × 7) and (b) Si(111)-(4 × 1)-In surfaces. Schematic drawing of Fermi surfaces of subbands of 2D quantum-well states and quasi-1D state are depicted left and right, respectively. (Lower) ARPES spectra for a 26-ML-thick Ag(111) film on Si(111)-(4 × 1)-In taken along the (c) $[1\bar{1}0]$ and (d) $[\bar{1}\,\bar{1}\,2]$ axes of the Si substrate.

the envelope function of a Bloch state perpendicular to the surface, $d$ is the film thickness, and $\phi_{vac}$ and $\phi_{sub}$ are the phase shifts at the film-vacuum and the film-substrate interface, respectively. For both substrates, energy positions of the quantized states systematically approach near $E_F$ with increasing film thickness [1,3,17,18]. The change leads one to extract the relation between $E_B$ and $k_z^{env}$ through the standard analyses of quantized states [5,13,17]. Figure 1(b) shows the experimental $k_z^{env}(E)$ values for the Ag films on the Si(111)-(4 × 1)-In surface. We have confirmed that the fitting function based on the two-band nearly free-electron model reproduces the Ag bulk band dispersion along the $\Gamma - L$ line, corresponding to the $z$ direction [5,13,17]. Comparisons of energy positions [Fig. 1(a)] and phase shifts [Fig. 1(c)] between Ag films on Si(111)-(7 × 7) and Si(111)-(4 × 1)-In substrates are described later.

Figures 2(a) and 2(b) show Fermi surfaces of quantized states in Ag films prepared on the two substrates mapped with photoemission intensity with an energy window of ±30 meV. For the Ag/Si(111)-(7 × 7) system in Fig. 2(a), the Fermi surfaces of a Ag(111) surface state (SS) and each subband of the quantized states are circles, indicating formation of isotropic two-dimensional (2D) free electrons, as expected. However, for the Ag/Si(111)-(4 × 1)-In system in Fig. 2(b), the Fermi surface of the SS is elliptical, and, furthermore, subbands of the quantized states are 1D lines parallel to the $k_x$ direction. To confirm the 1D feature, we present in Figs. 2(c) and 2(d) a series of photoemission spectra of Ag/Si(111)-(4 × 1)-In along (c) the $[1\bar{1}0]$ axis ($y$ direction) and (d) the $[\bar{1}\,\bar{1}\,2]$ axis ($x$ direction). As an emission angle changes from the surface normal, the energy positions of the quantized states approach $E_F$ along the $k_y$ axis, but they show no discernible dispersion along the $k_x$ axis. To elucidate the 1D anisotropy of in-plane band dispersion, $E_B - k_{x,y}$ diagrams created from Figs. 2(c) and 2(d) are shown in Figs. 3(a) and 3(b), respectively [6]. The subbands with parabolic dispersions are identified in the $E_B - k_y$ diagram along the $\bar{\Gamma} - \bar{K}$ ($k_y$ axis) direction as shown in Fig. 3(a). The dashed curves are parabolic fits [6,18] performed in the $k_y$ range from −0.2 to 0.2 Å$^{-1}$. The in-plane effective mass is $m_{\|}^* \sim 0.4m_e$, which is similar to the ones reported in the previous studies of quantum-well states [6,18]. On the other hand, the $E_B - k_x$ diagram along $\bar{\Gamma} - \bar{M}$ ($k_x$ axis), presented in Fig. 3(b), shows subbands with little dispersion.

To interpret the origins of the quasi-one-dimensionality of the quantized states in the epitaxial 2D film, we refer to the recent structure research on the present system. Uchihashi *et al.* [16] have found by scanning tunneling microscopy that the surface of an epitaxial Ag(111) film possesses a stripe structure with a period of 13.5(±0.8) Å parallel to the In chains. The stripe period corresponds to the spatial interval between the In chains, and it is commensurate to the bulk Ag fcc structure if stacking faults (plane defects across the film) exist at every sixth Ag atom along this direction. A cross section of the film is depicted in Fig. 4(a). The periodic stacking fault results in making the Ag film a superlattice structure with a unit cell of a parallelogram (base: the In chain interval 13.3 Å; height: the film thickness $d$). Therefore, the electronic property of the Ag film is no longer isotropic in the in-plane directions. The electron motion is free-electron-like along the $y$ direction while it is strongly perturbed in the $x$ direction. This is consistent with the experimental in-plane band dispersion (Figs. 2 and 3), and the quasi-1D feature implies that the superlattice structure [Fig. 4(a)] likely induces electron confinement between the stacking fault planes. We speculate that the confinement originates from electron interactions with a periodic potential (the Kronig-Penney-type potential) of the stacking faults. Here we make the following simple discussion in terms of the quantum size effect of a bulk Ag crystal.

For simplicity, instead of the structure model in Fig. 4(a), we assume that the unit cell of the superlattice is a rectangle (base: 13.3 Å; height: $d$) and the stacking faults run normal to the surface. Figures 4(b) and 4(c) illustrate the band diagrams for bulk Ag [$E(k^{3D})$], an isotropic 2D Ag(111) film [$E(k^{2D})$], and a quasi-1D Ag film [$E(k^{q-1D})$]. When the Ag(111) film is sufficiently thin, the $E(k^{3D})$ continuum along the $\Gamma - L$ direction ($z$ direction) is broken up and only wave vectors that satisfy the condition of the phase-shift accumulation [Eq. (1)] are allowed [left panel in Fig. 4(b)], which has been confirmed in Fig. 1(b). In such a 2D Ag film, the subband has discrete $k_z^{2D}$ values while it shows a parabolic (free-electron-like) dispersion along the $k_x^{2D}$ ($\bar{\Gamma} - \bar{M}$) and $k_y^{2D}$ ($\bar{\Gamma} - \bar{K}$) axes [right panel in Fig. 4(b)]. Such isotropic 2D Ag films are actually formed on Si(111)-(7 × 7) [Fig. 2(a)], Si(001)-(2 × 1), and Cu(111) surfaces [6,13,18].

On the other hand, the present Ag film consists of periodic potential modulations due to stacking faults in the $x$ direction. In the Kronig-Penney model, the dispersion widths of the original free-electron bands are reduced with the spatial width $a$ and the energy height $V$ of each potential barrier of the model [19]. The little band dispersion found in ARPES measurements along the $x$ direction (Figs. 2 and 3) experimentally indicates that the band width is smaller than the ARPES peak width of about 0.3 eV. Adopting the $\delta$ potential at each stacking fault plane, we found it requires $Va = S \sim 5$ eV · Å to reproduce the present experimental dispersion along this direction. In the $\delta$ potential model, one can derive the reflection phase

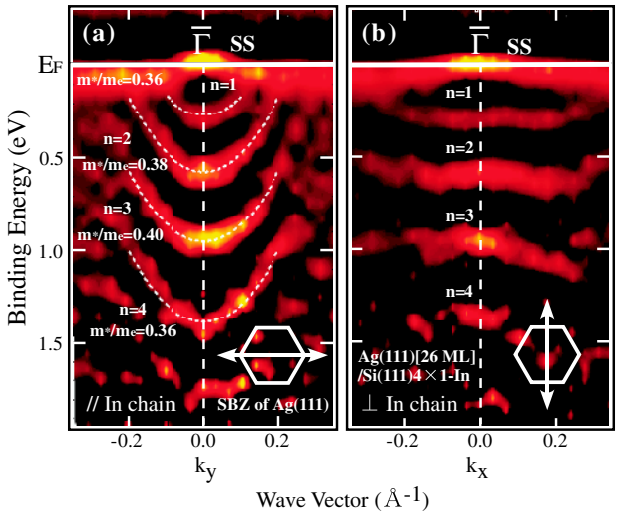


FIG. 3 (color online). The gray-scale $E_B - k_{x,y}$ diagram for the 26-ML-thick Ag(111) film on a Si(111)-(4 × 1)-In surface along the (a) Si(111)-(4 × 1)-In[$1\bar{1}0$] ($\parallel$ In chain) and (b) [$\bar{1}\,\bar{1}\,2$] ($\perp$ In chain) axes of the Si substrate taken from the ARPES scans shown in Fig. 2. The relation between the ARPES scan direction (arrow) and the surface Brillouin zone (SBZ) of Ag(111) is schematically indicated in the figure. The dashed lines are the parabolic fits of the dispersion curves for subbands, and the fitted in-plane effective mass $m_{\parallel}^*/m_e$ is indicated.

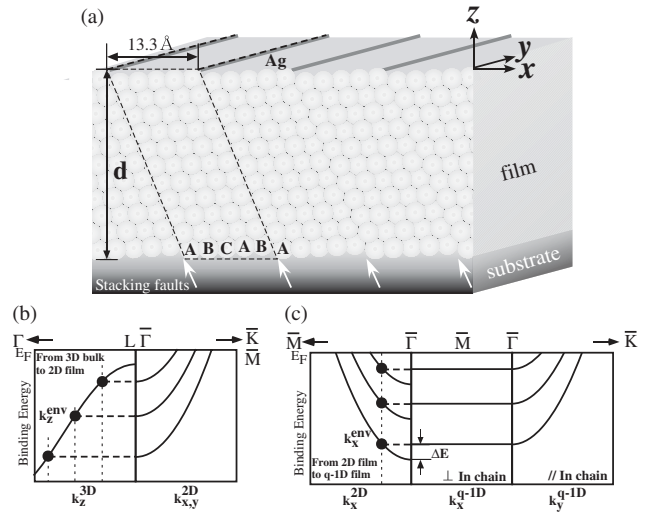


FIG. 4. (a) Cross sectional structure model for the Ag(111) film on Si(111)-(4 × 1)-In [16]. Locations of the stacking faults are indicated by arrows. Different alphabets are assigned for Ag atoms at different sites and a unit cell is indicated. (b) Schematic diagram describing discretization of the wave vector along the surface normal ($z$ direction, $\Gamma$-L direction) in an isotropic 2D film. The $\Gamma$-L line of bulk 3D Ag metal is projected to the $\bar{\Gamma}$ point ($k_{2D}^{x,y} = 0$) of the 2D Ag film. (c) Discretization of the wave vector perpendicular to the In chain ($x$ direction, $\bar{\Gamma} - \bar{M}$ direction). The binding energy of each subband at the $\bar{\Gamma}$ point for quasi-1D (q-1D) is smaller than that of the isotropic 2D film.

shift $\eta$ at the potential barrier at the stacking faults through the relation $\eta = \tan^{-1}(\hbar^2 k/Sm^*)$ [20]. Namely, we can apply a new boundary condition of the phase shift along the $x$ direction:

$$2k_x^{\mathrm{env}} b + 2\eta = 2\pi p, \tag{2}$$

where $p$ is the quantum number ($p > 0$), $k_x^{\mathrm{env}}$ is the wave vector of the envelope function of a Bloch state along the $x$ direction, and $b$ is a period of the potential (13.3 Å). Inserting the expression form of $\eta$ with $k = k_x^{\mathrm{env}}$ into Eq. (2), one finds the relation $\tan(k_x^{\mathrm{env}} d) = -\hbar^2 k_x^{\mathrm{env}}/Sm^*$, which yields $k_x^{\mathrm{env}} \sim 0.2$ Å$^{-1}$. It is noted that the value is similar to that of the hard wall model: $\pi/b = 0.24$ Å$^{-1}$. Contrary to the isotropic parabolic band dispersions for a 2D film, energy levels are allowed only for the ones with $k_x^{\mathrm{env}}$ for the quasi-1D case. Therefore, as shown in Fig. 4(c), each subband shows little band dispersion along the $k_x^{q-1\mathrm{D}}$ axis ($\bar{\Gamma} - \bar{M}$) while parabolic (free-electron-like) dispersion along $k_y^{q-1\mathrm{D}}$ ($\bar{\Gamma} - \bar{K}$), reproducing the experimental results in Fig. 3.

Through the reduction of dimensions from 2D to quasi-1D, the energy level (the band bottom) at the $\bar{\Gamma}$ point shifts to a smaller binding energy $\Delta E$ in Fig. 4(c). In the present case, it is estimated $\Delta E \sim 300$ meV. To confirm this energy change, let us now return to Fig. 1(a). Comparing the spectra between the two substrates, one recognizes that, at the same film thickness, subbands of the same quantum number show smaller $E_B$ at the $\bar{\Gamma}$ point for the quasi-1D Ag film on Si(111)-(4 × 1)-In than those of the isotropic 2D Ag film on Si(111)-(7 × 7). This experimental energy shift is 100–200 meV, and it is reasonably consistent to the $\Delta E$ value, estimated above, despite the very simple analysis. Namely, the experimental fact in Fig. 1(a) also indicates the formation of quasi-1D states in the Ag/Si(111)-(4 × 1)-In system.

Similar to the present case, there have been photoemission studies on 1D confinement of a 2D surface state by surface steps on a vicinal metal surface [21]. The researchers have found that only the lowest subband selectively appears at the normal emission of a surface terrace due to the photoemission matrix effect associated with symmetry (parity) of 1D wave functions. Therefore, it is most likely that the observed photoemission signals in Figs. 1–3 are assigned to the lowest 1D subbands of the original 2D bands. It explains naturally the absence of higher subbands in the present results, and, furthermore, it supports the aforementioned arguments of energy difference between the 2D and 1D bands.

Finally, we compared $\phi_{\mathrm{sub}}$ for the two underlying surface superstructures. The value of $\phi_{\mathrm{vac}} + \phi_{\mathrm{sub}}$ is directly obtained by inserting the energy dispersion $[k_z^{\mathrm{env}}(E)]$ in Fig. 1(b) to Eq. (1). In the WKB approximation [17], $\phi_{\mathrm{vac}}(E)$ is expressed as $\phi_{\mathrm{vac}}(E)/\pi = [3.4/(\Phi + E_B)]^{1/2} - 1$, where $\Phi$ is a work function of the Ag(111) surface (4.5 eV). Thus, the $\phi_{\mathrm{sub}}(E)$ values are obtained for the Ag/Si(111)-(7 × 7) and Ag/Si(111)-(4 × 1)-In systems as in Fig. 1(c). Within an experimental error, $\phi_{\mathrm{sub}}(E)$ of the two substrates are similar at $E_B = 0.7$–2 eV, but they are different from each other at $E_B < 0.7$ eV. The $\phi_{\mathrm{sub}}(E)$ deviation may be due to a difference in substrate band bending and/or in-plane symmetry in wave functions.

In conclusion, we have found the quasi-1D states in a Ag quantum film prepared on Si(111)-(4 × 1)-In through ARPES measurements of the quasi-1D Fermi surface, band dispersion, and the energy shift by the 1D electron confinement. We expect that these experimental results will stimulate research on interface structure analysis and theoretical calculations for the complete comprehension of the present topological phase transition [10].

We acknowledge C. Obuchi and M. Minowa for their helps. This work has been supported by Grants-In-Aid from the Japanese Society for the Promotion of Science.

*Electronic address: matsuda@surface.phys.s.u-tokyo.ac.jp

[1] J. J. Paggel, T. Miller, and T. C. Chiang, Science **283**, 1709 (1999).
[2] Y. Guo *et al.*, Science **306**, 1915 (2004).
[3] T. C. Chiang, Surf. Sci. Rep. **39**, 181 (2000).
[4] I. Vilfan *et al.*, Phys. Rev. B **66**, 241306(R) (2002).
[5] J. E. Ortega *et al.*, Surf. Rev. Lett. **4**, 361 (1997).
[6] I. Matsuda, T. Ohta, and H. W. Yeom, Phys. Rev. B **65**, 085327 (2002).
[7] L. Aballe *et al.*, Phys. Rev. Lett. **87**, 156801 (2001).
[8] S.-J. Tang, T. Miller, and T.-C. Chiang, Phys. Rev. Lett. **96**, 036802 (2006).
[9] P. Moras *et al.*, Phys. Rev. Lett. **96**, 156401 (2006).
[10] A. E. Meyerovich and D. Chen, Phys. Rev. B **66**, 235306 (2002).
[11] H. W. Yeom *et al.*, Phys. Rev. Lett. **82**, 4898 (1999).
[12] H. Morikawa, I. Matsuda, and S. Hasegawa, Phys. Rev. B **70**, 085412 (2004).
[13] A. Arranz *et al.*, Phys. Rev. B **65**, 195410 (2002).
[14] I. Matsuda *et al.*, Phys. Rev. B **71**, 235315 (2005).
[15] J. L. Lin *et al.*, J. Appl. Phys. **84**, 255 (1998).
[16] T. Uchihashi *et al.*, Phys. Rev. Lett. **96**, 136104 (2006).
[17] I. Matsuda *et al.*, Phys. Rev. B **63**, 125325 (2001).
[18] M. A. Mueller, T. Miller, and T.-C. Chiang, Phys. Rev. B **41**, 5214 (1990).
[19] C. Hamaguchi, *Basic Semiconductor Physics* (Springer-Verlag, Berlin, 2001).
[20] J. H. Davies, *The Physics of Low-Dimensional Semiconductors* (Cambridge University Press, Cambridge, England, 1998).
[21] A. Mugarza *et al.*, Phys. Rev. Lett. **87**, 107601 (2001); Phys. Rev. B **67**, 081404(R) (2003).